IEEE Access
Multidisciplinary | Rapid Review | Open Access Journal

Received August 9, 2020, accepted September 6, 2020, date of publication September 21, 2020,
date of current version September 29, 2020.

Digital Object Identifier 10.1109/ACCESS.2020.3025361

Experimental Investigation of Terahertz Scattering: A Study of Non-Gaussianity and Lateral Roughness Influence

MAI ALISSA[1], (Student Member, IEEE), BENEDIKT FRIEDERICH[2], FAWAD SHEIKH[1], (Member, IEEE), ANDREAS CZYLWIK[2], AND THOMAS KAISER[1], (Senior Member, IEEE)

[1]Institute of Digital Signal Processing, University of Duisburg-Essen, 47057 Duisburg, Germany
[2]Chair of Communication Systems, University of Duisburg-Essen, 47057 Duisburg, Germany

Corresponding author: Mai Alissa (mai.alissa@uni-due.de)

This work was supported in part by the Deutsche Forschungsgemeinschaft (DFG) Priority Programme Schwerpunktprogramm (SPP) 1655 (Wireless 100 Gb/s and beyond) through the Project Tera50, and in part by the Deutsche Forschungsgemeinschaft (DFG, German Research Foundation) through Project M01 under Project - ID 287022738 - TRR 196.

ABSTRACT The scattering phenomenon caused by rough surfaces has a dominant role in shaping the reflected field at terahertz (THz) frequencies, both in specular and non-specular directions. Most surfaces in nature are randomly rough, and the surface height obeys a certain statistical distribution. A Gaussian probability density function (PDF) for height distribution is often considered, and the correlation length is assumed to be longer than the wavelength. However, a clear understanding of how changing these assumptions affect the angular distribution of the scattered field is still lacking. In the first part of this work we investigate via microscopic measurements the statistical distribution of realistic indoor materials, and its deviation from the assumed normal distribution. After that, the influence of non-Gaussianity on the specular reflection in the low THz region is shown analytically. In the second part, a measurement campaign of diffuse scattering, caused by structured statistically-controlled surfaces, is reported. The correlation length assumption has been proven experimentally and via full-wave simulation to affect the diffuse scattering by rough samples, when the other statistical parameters are kept without changes.

INDEX TERMS THz communication, scattering measurements, statistically-controlled rough surfaces, non-Gaussian heights' distributions.

I. INTRODUCTION

Global mobile data traffic is expected to exceed 77 exabytes per month by 2022 [1], which is more than double the data traffic in 2019. In order to fulfill such extreme data rate demands, the carrier frequencies of wireless links need to be expanded into higher ranges beyond 100 GHz. Due to the abundant availability of bandwidth, terahertz (THz) wave technologies are proposed as one of the key fields of wireless communications for 5G and beyond. Although THz applications have already reached maturity in some fields of science, like astrophysics and imaging, THz frequency range is one of the least investigated regions of the electromagnetic spectrum for wireless communications. Very high propagation losses confine communication applications at THz frequencies and restrict them to short-range links in indoor environments [2]. Nevertheless, advances with respect to the generation of extremely high power THz waves [3] give a good indication that communications with THz signals are becoming more and more feasible. This is also reflected in the establishment of a new IEEE standard (IEEE 802.15.3 d standard) [4]. Here, a portion from the low THz band (252 to 325 GHz) was assigned to upcoming wireless communication links.

One significant difference of THz propagation compared to the currently allocated frequencies is the scattering phenomenon that appears due to the roughness of indoor surfaces. Material roughness determines the degree of scattering that occurs, with several parameters contributing to a specific distribution of the scattered rays. The non-specular scattering in the indoor environment causes a major multi-path

The associate editor coordinating the review of this manuscript and approving it for publication was Santi C. Pavone.

contribution and thus has a significant impact on propagation characteristics, primarily in the absence of a direct propagation link [5]. Empirical methods have been suggested to estimate the distribution of the scattered field. For example, in [6], the effective roughness (E-R) model was developed. Here, the field distribution in the angular domain is approximated by assuming a Lambertian scattering pattern and developed later to a directive pattern. However, such models characterize roughness by only measuring or estimating one single parameter, the surface heights' standard deviation.

Moreover, given the lack of a closed-form solution for the scattering problem, the effect of scattering is also included in ray-tracing models by employing analytical approximations. The most utilized method is the physical optics (PO), also known as the Kirchhoff approximation (KA). Scattering from surfaces obeying the KA was comprehensively investigated [5], [7]–[9]. In [5], the Beckmann-Kirchhoff (B-K) model, which is an advanced form of the KA, was implemented in these scattering models. The authors showed that the diffuse scattered power has a substantial impact on the non-line-of-sight (NLOS) propagation paths. A comparison between the E-R method and the B-K model for THz propagation has been described in [9].

When applying the Kirchhoff model, it has been assumed in all the previous studies that the surface heights follow a Gaussian distribution. The reason behind this assumption is apparent, and thus significantly reducing the complexity of the scattering problem, as the slope distribution function can be obtained directly. In reality, no surface is normally distributed all in all, and minimal attempt is made to characterize the roughness distribution of real surfaces and their deviation from normality. In an original paper from Beckmann [10], the scattered field from a normally distributed surface was compared to an exponentially-distributed one possessing the same standard deviations of heights. The scattering was significantly different, even for the specular direction, except for a slightly rough surface. The deviation has also been confirmed analytically in the optical domain, even for moderately rough surfaces [11]. To what extent does the surface height distribution of real materials fit a Gaussian distribution? How does the randomness assumption affect scattering behavior? These two questions are addressed in the first part of this work.

Another mandatory assumption for applying the B-K model is that the surface is locally smooth, i.e., the correlation length of the surface is greater than the wavelength of the electromagnetic wave [5]. The surface correlation length is a spatial roughness parameter and generally defined as the distance at which the surface autocorrelation function falls to $1/e$ of its maximal value. The assumption mentioned above may not be valid in real materials. For example, in [12], the correlation length of the two examined materials was 0.18 mm and 0.29 mm. If we consider a THz wave with a central frequency of 300 GHz, the correlation length in both cases is less than a third of the wavelength. Until today, experimental investigations about scattering, especially in the THz range, from rough surfaces, are very scarce. Reflection scattering measurements in the millimeter-wave range in [13] show that material surfaces exhibiting a roughness standard deviation equal to or greater than 0.3 mm induce a distinct influence on the roughness dependent power reduction of the reflected ray. In [14], [15], measurements of diffuse scattering at THz were reported. Here, sandpapers with different grit sizes were chosen to represent different levels of roughness. The authors in [7] proved experimentally that non-specular NLOS paths play a valuable role in enabling THz wireless links.

It is worth mentioning that since a rough surface is generated from a random process, the field scattered will be a random process. Therefore, measurement of the scattered field from one realization of a random surface is not enough to draw a conclusion about the scattering behavior, and therefore better estimated by an analytical model. In case we aim to investigate the lateral correlation effect, the statistics condition will be fulfilled if the sample size is much larger than the correlation length.

The second part of this work is dedicated to the study of correlation length assumption and its effect on the diffuse scattering profile. This is carried out via bistatic full-wave simulations and scattering measurements on constructed rough materials. The statistical parameters of the samples are monitored and realized by high accuracy photolithographic techniques.

II. MEASUREMENTS OF THE SURFACE STATISTICS OF REAL INDOOR MATERIALS

A. ROUGHNESS CHARACTERIZATION

A random rough surface is given by the function $\boldsymbol{h} = \boldsymbol{f}(x, y)$, where $\boldsymbol{h}$ is the surface height at a point (x, y). It is commonly described in statistical terms using two distribution functions, the heights' probability distribution, and the autocorrelation function. The heights' probability density function describes the surface height deviation from a certain mean level and the autocorrelation function describes the Δx from each other.

$$R_{hh}(\Delta x) = \mathbb{E}[h(x, y) * h(x + \Delta x, y)]. \tag{1}$$

The shape of the probability density function provides meaningful information about the nature of roughness, and the shape is described mathematically by an infinite number of higher moments, and approximated by the first four moments of the random process $\boldsymbol{h}$ in case of surface characterization. The first moment is the average heights, and it is calculated as

$$\bar{h} = \mathbb{E}[\boldsymbol{h}] = \int_{-\infty}^{\infty} h f_h(h) \mathrm{d}h \tag{2}$$

The second central moment is one of the most vital parameters to characterize roughness. The root mean square height is calculated by

$$\sigma = \sqrt{\mathbb{E}[(\boldsymbol{h} - \bar{h})^2]} = \int_{-\infty}^{\infty} (h - \bar{h})^2 f_h(h) \mathrm{d}h \tag{3}$$

The third central moment of the heights' distribution determines the skewness, it represents the asymmetric spread of

heights' distribution.

$$S_k = \mathbb{E}[\frac{(\boldsymbol{h} - \bar{h})^3}{\sigma^3}] = \int_{-\infty}^{\infty} \frac{1}{\sigma^3}(h - \bar{h})^3 f_h(h)\mathrm{d}h \quad (4)$$

The fourth central moment of the heights' distribution determines the kurtosis, and it represents the spikiness of the statistical distribution,

$$K_u = \mathbb{E}[\frac{(\boldsymbol{h} - \bar{h})^4}{\sigma^4}] = \int_{-\infty}^{\infty} \frac{1}{\sigma^4}(h - \bar{h})^4 f_h(h)\mathrm{d}h \quad (5)$$

In 2002, a working group (TC213/N499) was created aiming to develop international standards for surface characterization. The standard ISO 25178 was then released in 2005 [16]. The first-order moment is the average surface height. Assuming that the random height is an ergodic process, estimates of the moments can be calculated by averaging with respect to the area of a sample A. The second, third and fourth heights' parameters are defined as follows:

- Estimated average height ($\widetilde{\bar{h}}$)

$$\widetilde{\bar{h}} = \frac{1}{A}\iint_A \boldsymbol{h}(x, y)\mathrm{d}x\mathrm{d}y \quad (6)$$

- Estimated root mean square height ($\widetilde{\sigma}$)

$$\widetilde{\sigma} = \sqrt{\frac{1}{A}\iint_A (\boldsymbol{h}(x, y) - \widetilde{\bar{h}})^2\mathrm{d}x\mathrm{d}y} \quad (7)$$

σ is the only parameter of roughness necessary for calculating the Rayleigh parameter, which is one of the most applied criteria in determining if the surface is considered to be rough in scattering models. The Rayleigh parameter is given as

$$g = \left(\frac{4\pi\sigma\cos(\Theta_i)}{\lambda}\right)^2 \quad (8)$$

where Θ_i is the angle of incidence of the electromagnetic wave and λ is the wavelength.

- Estimated skewness ($\widetilde{S}_k$)
The skewness value within a given limited area is estimated by

$$\widetilde{S}_k = \frac{1}{A}\iint_A \frac{(\boldsymbol{h}(x, y) - \widetilde{\bar{h}})^3}{\widetilde{\sigma}^3}\mathrm{d}x\mathrm{d}y \quad (9)$$

Surfaces with high peaks and shallow valleys have positive values of skewness and vise versa. Symmetrical distribution functions, including Gaussian ones, have zero skewness.

- Estimated Kurtosis ($\widetilde{K}_u$)
Similarly, the fourth moment is estimated as

$$\widetilde{K}_u = \frac{1}{A}\iint_A \frac{(\boldsymbol{h}(x, y) - \widetilde{\bar{h}})^4}{\widetilde{\sigma}^4}\mathrm{d}x\mathrm{d}y \quad (10)$$

TABLE 1. A list of the investigated materials, with the measured areas and the heights standard deviations.

Material	Symbol	Measured Area	σ (mm)
Dark Oak	A2	35 mm x 35 mm	0.047
Laminate	A3	35 mm x 35 mm	0.052
Brick	B1	35 mm x 35 mm	0.095
Leather	L1	15 mm x 15 mm	0.049
Leather	L2	35 mm x 35 mm	0.031
Wood	W1	15 mm x 15 mm	0.047
Wood	W2	35 mm x 35 mm	0.050
Wood	W5	35 mm x 35 mm	0.012
Wood	W6	35 mm x 35 mm	0.029
Wall Paper	WP1	35 mm x 35 mm	0.145
Wall Paper	WP2	35 mm x 35 mm	0.085
Wall Paper	WP3	35 mm x 35 mm	0.074
Wall Paper	WP6	35 mm x 35 mm	0.131
MDF	P3	35 mm x 35 mm	0.013
MDF	P4	35 mm x 35 mm	0.005

When $K_u > 3$ the statistical distribution has a distinct peak, and the higher K_u is the sharper the peak becomes. Values of $K_u < 3$ indicate a rather flat distribution.

B. METHODS AND MATERIALS

For standard measurements of roughness, two main methods can be applied, linear or aerial surface roughness measurements. A linear roughness measurement system investigates roughness in two dimensions (x,y) in the form of single lines. In contrast, an areal three dimensional (3D) roughness measurement is conducted over an area of the surface.

In this work, the latter method is used in the form of a high accuracy non-contact laser confocal microscopy system. With confocal microscopy, it is possible to investigate the three dimensional surface structures at sub-micron resolutions. A sequence of digital images is acquired for each sample. Then, the output stack of photos is post-processed with the surface metrology software MountainsMap [17]. The reconstructed 3D model is a digital image representing the surface, where each pixel has a value that refers to the surface height. Based on the reconstructed 3D model, the four surface heights parameters, as defined by the ISO 25178 standard and described in section II. A, are then calculated.

In this study, real materials, which are commonly found in an indoor environment, are investigated. Table 1 lists the 15 investigated material, including their measured areas and root mean square heights σ. The maximum patch area that can be measured by the confocal microscopy is 7 mm x 7 mm. For each material, five patches of 7 mm x 7 mm were measured at statistically independent positions, S_k and K_u parameters are then averaged over the repeated measurements. Only in two cases (L1, W1), the resumed area size is 3 mm x 3 mm.

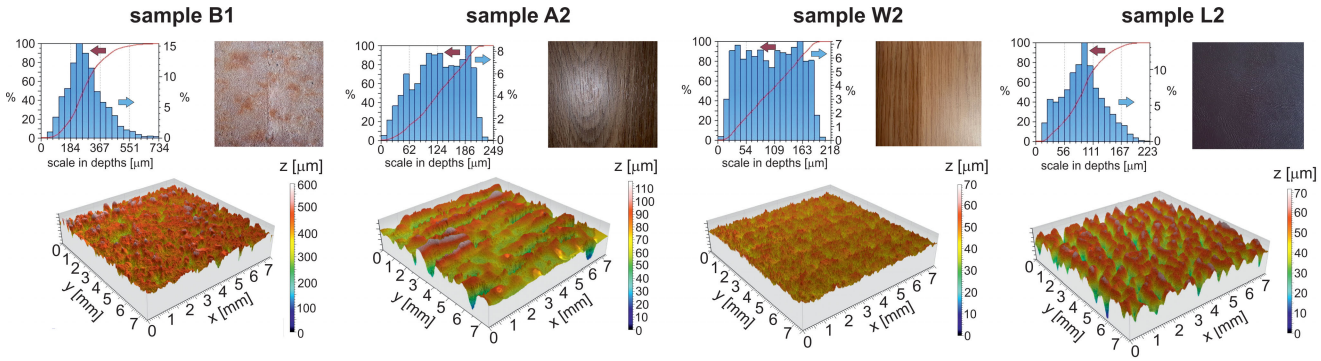

FIGURE 1. The measured statistical distributions of four selected samples in the form of histograms (upper part) and surface 3D maps (lower part), demonstrating the non-Gaussian nature of the real rough surfaces.

C. MEASUREMENTS RESULTS

Representative surface maps and histograms of four samples (B1, A2, W2, L2) are obtained from the aforementioned measurements and post-processing procedure. The results are displayed in figure 1. As can be seen from the histograms, some real surfaces do not follow Gaussian heights' distribution. For example, comparing the surface maps and histograms of sample A2 and W2 indicates that two different materials have completely different surface structures, even if their height standard deviations are comparable. The last column of Table 1 presents the calculated standard deviation of the surface heights, ranging between 0.005 mm for the smoothest sample and 0.145 mm for the roughest one.

In figure 2, the calculated skewness and kurtosis values are represented as blue dots for all the samples. The blue bars in both x and y directions represent the error caused by averaging over the repeated measurements. The red dot in this figure has skewness $S_k = 0$ and kurtosis $K_u = 3$, which represents the Gaussian distribution. The green dot represents a Gamma distribution of the fourth degree ($\kappa = 4$), which has skewness value of $S_k = 1$ and kurtosis $K_u = 4.5$. Note that the exponential distribution, which is most compared to the Gaussian in older studies, has very extreme values ($S_k = 2$, $K_u = 9$), and is not close to any of the measured real materials, so we did not include it in this figure.

Most of the investigated materials tend to have a skewness value between -0.5 and 0.5, and the kurtosis values are closer to 2 than 3.

Four samples (B1, W5, WP2, WP3) have more extreme values of S_k and K_u and their deviations from a normal distribution is obvious, WP2 and WP3 could be better represented by a Gamma distribution. In the following section, we will check analytically the effect of the deviation from the assumed Gaussian distribution due to the scattering, within our frequency range of interest.

D. ANALYTICAL DESCRIPTION OF THE SCATTERING

In this section, the general theory of scattering by random rough surfaces, described in [18], is adopted. The surface is assumed homogeneous and continuous, with an average

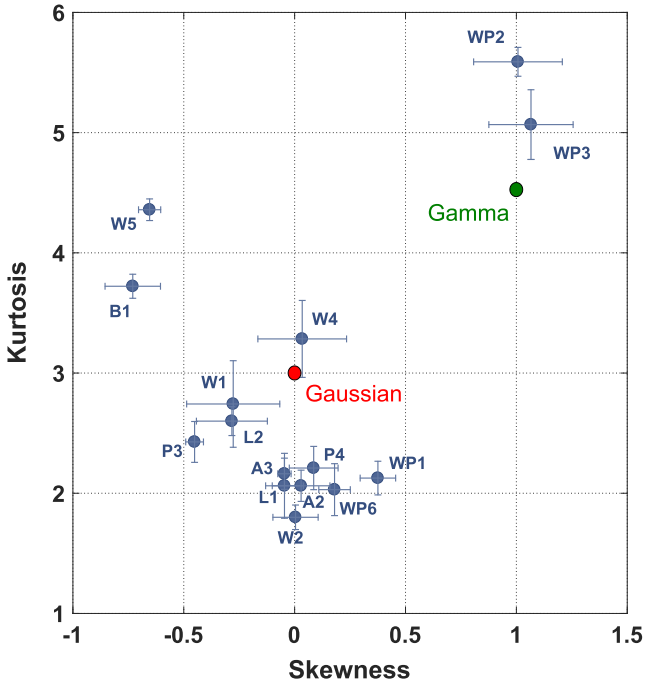

FIGURE 2. Measured skewness and kurtosis of the investigated indoor samples, the red spot represents the Gaussian case, Gamma from the fourth degree is shown in green.

surface height equal to zero. The surface height is a random field. The specular reflection factor depends on $\boldsymbol{k}$, and is given as in [18]

$$S_{\text{spec}}(k_\perp) = \frac{I_{\text{spec}}}{I_{\text{tot}}} = \left| \int f_h(h) \mathrm{e}^{jk_\perp h} \mathrm{d}h \right|^2 \tag{11}$$

where I_{tot} is the total integrated intensity of the reflected and scattered fields, and I_{spec} is the intensity of the specular direction. The specular reflection factor has a direct relation to the surface heights' probability density function.

E. THE GAUSSIAN CASE

For a random surface with a surface height that follows the Gaussian distribution, the PDF of the surface height is given

by

$$f_{h,\text{Gauss}}(h) = \frac{1}{\sqrt{2\pi}\sigma} e^{-h^2/2\sigma^2} \tag{12}$$

By employing in relation (11), the specular reflection factor for the Gaussian case is

$$S_{\text{spec, Gauss}}(k_\perp) = e^{-k_\perp^2\sigma^2}, \tag{13}$$

F. THE NON-GAUSSIAN CASE

The specular reflection factor can be calculated if $f_h(h)$ is known as mentioned in equation (11). A non-Gaussian surface refers to a very general case as any surface which does not follow the normality assumption is non-Gaussian. Here, we will give two examples of non-Gaussian surfaces and calculate the expected specular scattered intensity. The first is the exponential distribution ($S_k = 2, K_u = 9$), one of the most compared to the Gaussian in previous works. The second is the Gamma distribution of the fourth degree ($S_k = 1$, $K_u = 4.5$), which fits well to some of the measured samples, as mentioned in the previous section. An exponential distribution has the following form [18]

$$f_{h,\text{exp}}(h) = \frac{1}{\sigma}\left(e^{\frac{-h}{\sigma}}\right) \tag{14}$$

while the Gamma distribution is modeled as in [18]

$$f_{h,\text{gamma}}(h) = \frac{1}{\Gamma(\kappa+1)\sigma^{\kappa+1}} h^\kappa \left(e^{\frac{-h}{\sigma}}\right) \tag{15}$$

Integrating into equation (11), the specular reflection factor from an exponentially distributed surface is given by

$$S_{\text{spec,exp}}(k_\perp) = \frac{1}{1+k_\perp^2\sigma^2}, \tag{16}$$

The specular reflection factor for Gamma distributed surface is then calculated as

$$S_{\text{spec,gamma}}(k_\perp) = \frac{1}{(1+k_\perp^2\sigma^2)^{\kappa+1}}, \tag{17}$$

By evaluating equations (13), (16) and (17) numerically, the intensity of the scattered field in the specular direction is calculated for the three statistically different surfaces. Figure 3 shows the different curves of specular reflection factor with respect to increasing the heights' standard deviation σ at a normal incident angle with a carrier frequency of 300 GHz. From figure 3, we notice that the assumption of a Gaussian height distribution underestimates the reflected signal in the specular direction for large values of σ. Already for $\sigma = 0.2$ mm the specular reflection component in case of the Gamma distribution is by 4 orders of magnitude larger than assuming a Gaussian distribution. Moreover, the exponential distribution shows a similar specular intensity like the Gaussian one for low values of σ, but exhibits a much higher specular intensity for very rough surfaces where σ reaches the wavelength of the incident wave. Nevertheless, if we take a look back at the measured materials, the roughest material has a standard deviation of heights equal to 0.0145 mm.

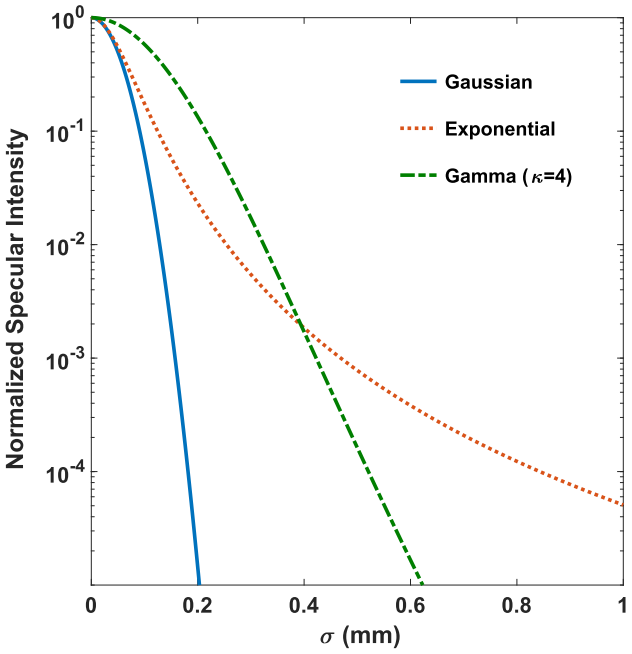

FIGURE 3. Analytical calculation of the specular scattered intensity for three different statistical distributions of the surface heights with increasing σ. The carrier frequency is 300 GHz at a normal incident angle.

At a 300 GHz carrier frequency, the deviation in the specular intensity, caused by changing the distribution, is small and can be neglected. In other words, the Gaussian distribution is still valid even when the real statistics of the material differ from Gaussian. This is true for low THz frequencies, which attracts our interest in this study. Note that the important factor here is the ratio between σ and the wavelength λ. Changing the frequency to a higher level has the same effect as increasing σ, and the surface distribution assumption is expected to have a noticeable deviation in the scattered intensity.

III. EXPERIMENTAL MEASUREMENTS ON THz SCATTERING BY ROUGH CONTROLLED SAMPLES

The aim of this section is to investigate the THz wave scattering by 3D printed samples with defined surface statistical parameters. The resulting measurements can then be used to develop a better understanding of how the correlation length assumptions affect the accuracy of THz propagation models.

A. SAMPLE PREPARATION

The numerical generation of random surfaces with specific roughness parameters is well studied in the literature. Here, we adopted a spectral method similar to the one described in [19]. A random rough surface with the desired properties is generated starting with generating an uncorrelated Gaussian random rough surface distribution using a Gaussian random number generator, with an average of zero and different standard deviations σ. To achieve a correlation of surface points, the distribution is then convolved with correlation

function having an exact value of the correlation length. This can be implemented numerically by applying a Fast Fourier Transform (FFT).

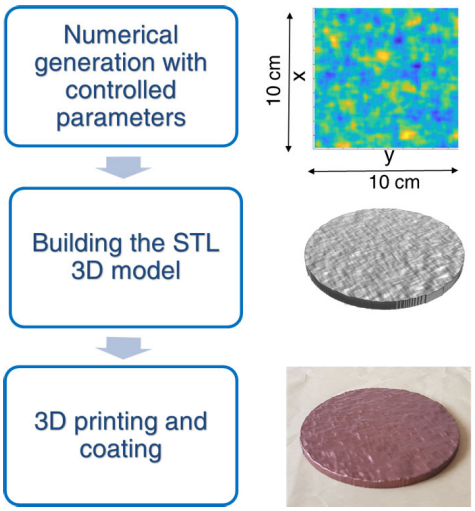

FIGURE 4. The required steps for obtaining rough samples with controlled statistics.

The samples are then exported as standard tessellation language (STL) three dimensional (3D) models. The models are printed following Stereolithography (SLA) 3D printing method. SLA provides a high vertical resolution of 25 microns. The material used is standard Resin. The steps for obtaining rough samples with controlled statistics are depicted in figure 4.

The dimensions of the discussed surfaces are 100 mm x 100 mm x ($5 \pm \sigma$) mm (length x width x height). Finally, a layer of pure copper (99.9% copper) is applied to prevent the scattering inside the material, and the copper can be considered as perfectly conducting material at low THz frequencies. The layer thickness of the coating is not known accurately but is significantly thin, so it does not affect the surface statistics. A representation of a numerical 3D generated surface, the STL model and the realized 3D sample are shown in figure 4. Table 2 provides presumed and actual statistical parameters of the printed samples, the S0 sample is a smooth surface having the same size and coated with copper.

TABLE 2. The assumed and real values of the statistical parameters for the 3D printed samples.

	S0	S1	S2	S3	S4
σ **assumed (mm)**	-	0.150	0.150	0.150	1.000
σ **actual (mm)**	-	0.151	0.148	0.153	1.012
l_c **assumed (mm)**	-	0.30	1.30	3.00	1.30
l_c **actual (mm)**	-	0.30	1.32	2.94	1.31

B. MEASUREMENT SETUP

The measurement setup, shown in figure 5, was used to calculate the bistatic angular distribution of the THz signal

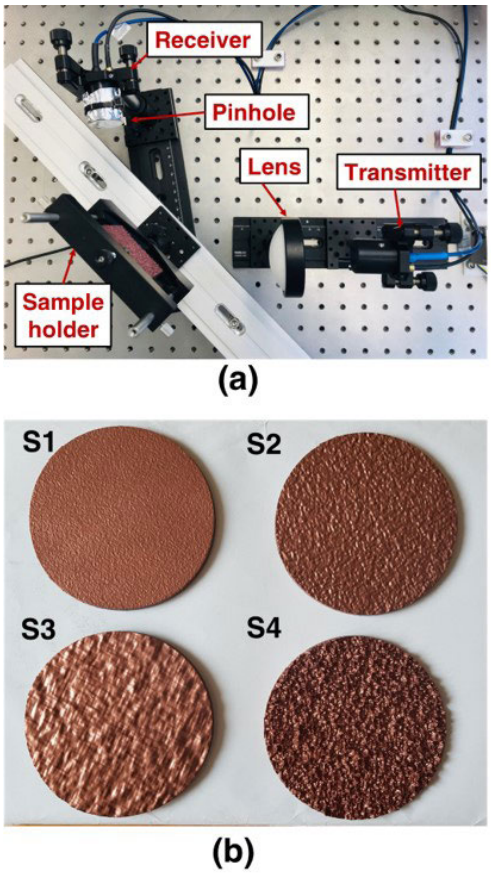

FIGURE 5. (a) Measurements setup for obtaining the diffuse scattering by the 3D printed rough samples. (b) a photo of the realized 3D printed rough samples.

scattered by the rough samples. The Frequency-domain terahertz platform (i.e., THz-FDS), with 40 MHz frequency resolution, is used to generate the THz incident signal. The transmitter is a continuous-wave THz transmitter, consists of photodiode coupled with integrated antenna and a silicon lens.

The THz signal emitted by the transmitter is collimated with a 2" PTFE lens with a back focal length of 63.2 mm. The lens is placed 100 mm from the center of the sample and the angle of incidence is fixed at $\theta_i = 22°$. The lens assures that the collimated THz beam becomes nearly a plane wave. The THz receiver is made of an antenna-integrated photo-conductor with a silicon lens and is placed over a motorized rotation stage. Moreover, a pinhole with a diameter of circa 1 mm is placed in front of the lens, the pinhole eliminates angular dependence of the radiation pattern on the receiver and rises the spatial resolution. The receive antenna is placed 100 mm away from the rotation center, and by rotating the rotation stage, the receiver antenna rotates on a circular track around the sample, in the range between 60° and 0° with a step of 1°. The observation angle is considered relative to the angle under which the specular reflection is estimated.

C. RESULTS AND DISCUSSIONS

Figure 6 and 7 present examples of the scattering by rough samples in the form of bistatic radar cross section (RCS) full-wave simulation for a specific frequency (300 GHz) with a normal incident angle. The blue curve in both figures represents the normalized RCS in the case of a smooth perfectly conductive surface, whereas rough surface RCS values are calculated from 10 realizations of each rough sample and then normalized according to the peak of the blue curve, which is the specular reflection. In Figure 6, the rough sample standard deviation is similar to the maximum value of a normal indoor real material, and the correlation length has the value of three times the wavelength $l > \lambda$, i.e., the values which are frequently assumed when applying KA. Compared to the smooth surface, a degradation of around 20 dB is observed in the specular reflection, and the strongest side lobe of the diffuse scatter in around 15 dB less than the specular reflection. The diffuse scattering effect is evident in the non specular angles, and it is around (20-30) dB higher compared to the smooth surface reflection in the range $-50°$to $50°$ around the specular.

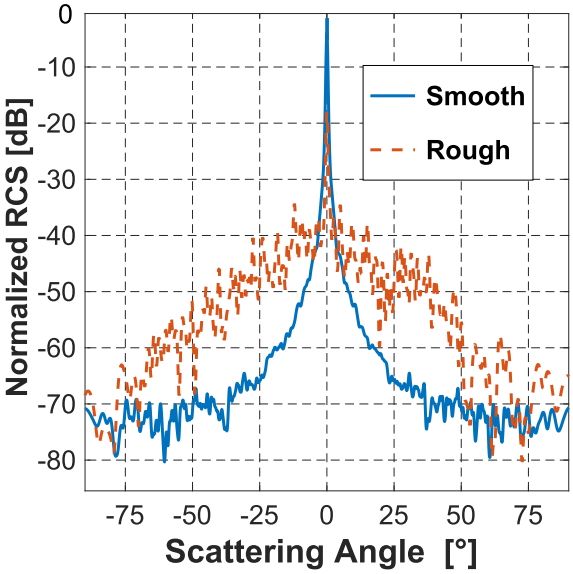

FIGURE 6. Bistatic RCS simulation of scattering by a controlled rough surface versus a smooth surface ($\sigma = 0.15$ mm, $l_c = 3$ mm) at 300 GHz, for a normal angle of incidence, computed using plane wave-full simulation.

In figure 7, the rough sample has the same heights' standard deviation, but a shorter correlation length $l < \lambda$. In this case, the reflected specular power degradation is 10 dB, with a small amount of diffuse scattering outside the specular direction. It appears that although samples in figure 6 and 7 differ only in the lateral correlation length, and the rest of the statistical parameters are the same, the scattered field distribution is different. The sample with a correlation length shorter than the wavelength acted more like a smooth surface, and the reflection is more specular. The measured and simulated RCS of samples S0, S1, S3, and S4 are depicted in figure 8 for an incident angle of 22° and frequency range

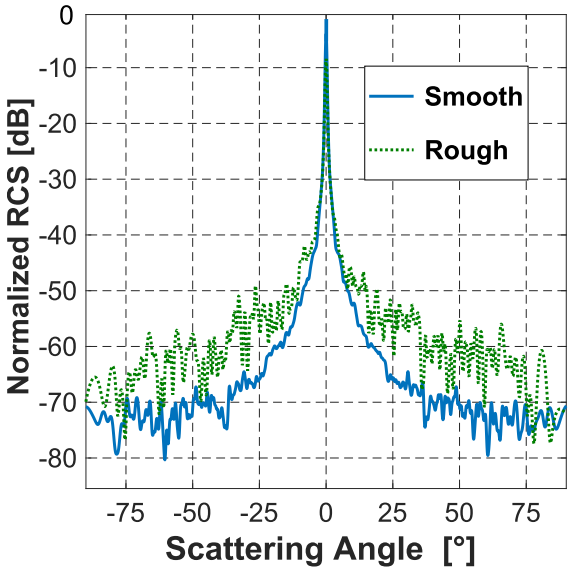

FIGURE 7. Bistatic RCS simulation of scattering by a controlled rough surface ($\sigma = 0.15$ mm, $l_c = 0.3$ mm) versus a smooth surface at 300 GHz, for a normal angle of incidence, computed using plane wave-full simulation. Note the effect of decreasing the correlation length.

200 to 400 GHz. In the worst case, at 200 GHz, the ratio of the surface diameter to the wavelength is 66.7. A good agreement is found between the plane wave scattering simulation and the real measurements. The scattering angular distribution of the two samples where the correlation is longer than the wavelength (S2 and S3) shows no noticeable difference. Thus, S3 angular scattering is only shown. The reflection by smooth surface S0, shown in figure 8 (a) and (b) causes a clear specular narrow peak in the complete range of frequency, with a slight decrease of specularly reflected power close to 400 GHz. A comparison between measurements results in figure 8 (c) and (e), and also full-wave simulation in the same figure (d) and (f), indicates that a correlation length shorter than the wavelength makes a surface with fixed roughness height's standard deviation more similar to a smooth reflector. Thus, it increases the specular reflection at a given frequency. The previous effect of the correlation is dominant for slightly rough surfaces. In the case of highly rough materials, the specular reflection is completely destroyed, and the power is scattered randomly all over the angular field. Figure 8 (g) and (h) depict an example of how a very rough sample, S4 here, would destroy the specular reflection.

In order to keep the comparison fair, this study is limited to perfectly conducting samples. No parameters regarding the nature of the surface were included, such as its permittivity and conductivity. However, it would be interesting to calculate the RCS of rough samples considering also these two parameters. The metal coverage of the samples incurs a complete reflection of the waves, without losses inside the material. A further investigation of dielectric samples, with several values of permittivity and conductivity, is planned to follow this work.

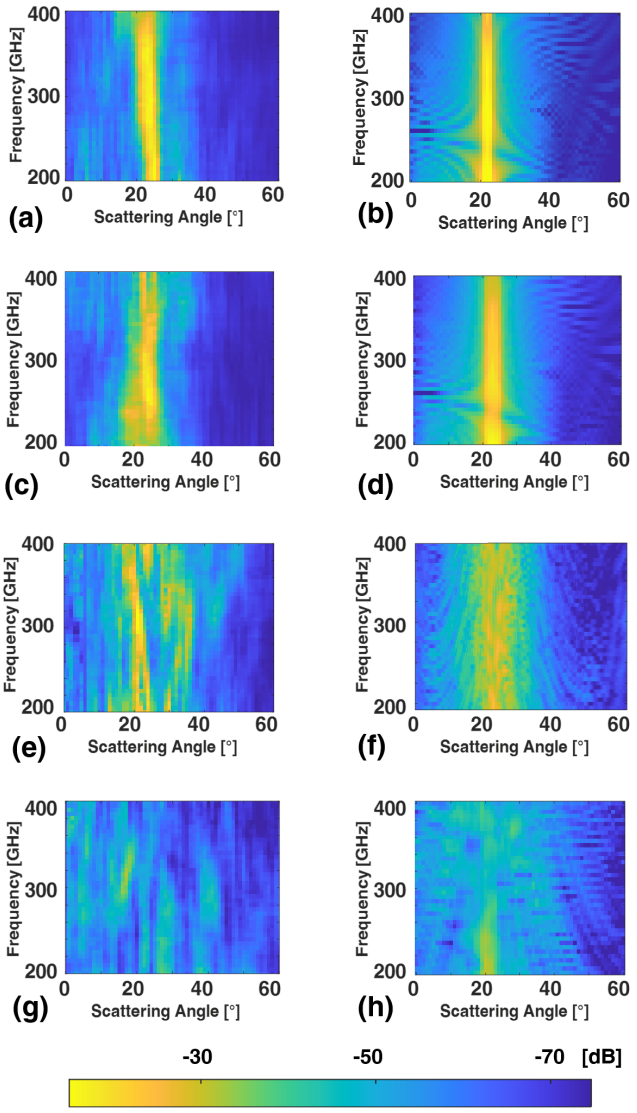

FIGURE 8. Measured and simulated scattering coefficient normalized by the maximum value of scattering by a smooth surface for: (a) S0 measurements, (b) S0 simulated,(c) S1 measurements, (d) S1 simulated,(e) S3 measurements, (f) S3 simulated, (g) S4 measurements, (h) S4 simulated.

IV. CONCLUSION AND FUTURE WORK

We report measurements-based investigation to validate two assumptions, which are commonly adopted when calculating the scattered field distribution by Kirchhoff analytical approximation. First, real statistical distributions of rough indoor materials are measured, and their deviations from the assumed Gaussian distribution are calculated. Thereafter, an analytical study of specular scattering with changing the Gaussian assumption is conducted. We conclude that the distribution assumption has a minor effect in the lower THz band, within the limits of real indoor materials. However, a Gaussian height distribution significantly underestimates the measured signal in the specular direction for large values of the surface heights' standard deviation compared to the wavelength. This indicates that the assumption has no effect only in lower THz band, but such an assumption should be avoided in case of higher frequencies. Statistically controlled rough samples are designed and fabricated, and measurements were also performed on the manufactured samples to inspect the effect of alterations in the rough sample correlation length. If the surface correlation length is larger than the wavelength, the diffuse scattering caused by the surface roughness increases drastically. It is observed that when such a condition is not fulfilled, the rough surface causes more reflection, taking the specularity roll-off to higher frequencies. We believe that the obtained results act as an advanced step in developing realistic models for angular distribution of the scattered fields in the THz band.

REFERENCES

[1] *Cisco Annual Internet Report (2018–2023) White Paper*. [Online]. Available: https://www.cisco.com

[2] I. F. Akyildiz, C. Han, and S. Nie, "Combating the distance problem in the millimeter wave and terahertz frequency bands," *IEEE Commun. Mag.*, vol. 56, no. 6, pp. 102–108, Jun. 2018.

[3] A. D. Koulouklidis, C. Gollner, V. Shumakova, V. Y. Fedorov, A. Pugžlys, A. Baltuáka, and S. Tzortzakis, "Observation of extremely efficient terahertz generation from mid-infrared two-color laser filaments," *Nature Commun.*, vol. 11, no. 1, Dec. 2020, Art. no. 292, doi: 10.1038/s41467-019-14206-x.

[4] *IEEE Standard for High Data Rate Wireless Multi-Media Networks–Amendment 2: 100 Gb/s Wireless Switched Point-to-Point Physical Layer*, Standard802.15.3d-2017, Oct. 2017.

[5] R. Piesiewicz, C. Jansen, D. Mittleman, T. Kleine-Ostmann, M. Koch, and T. Kurner, "Scattering analysis for the modeling of THz communication systems," *IEEE Trans. Antennas Propag.*, vol. 55, no. 11, pp. 3002–3009, Nov. 2007.

[6] V. Degli-Esposti, D. Guiducci, A. de'Marsi, P. Azzi, and F. Fuschini, "An advanced field prediction model including diffuse scattering," *IEEE Trans. Antennas Propag.*, vol. 52, no. 7, pp. 1717–1728, Jul. 2004.

[7] J. Ma, R. Shrestha, W. Zhang, L. Moeller, and D. M. Mittleman, "Terahertz wireless links using diffuse scattering from rough surfaces," *IEEE Trans. THz Sci. Technol.*, vol. 9, no. 5, pp. 463–470, Sep. 2019.

[8] F. Sheikh, D. Lessy, and T. Kaiser, "A novel ray-tracing algorithm for non-specular diffuse scattered rays at terahertz frequencies," in *Proc. 1st Int. Workshop Mobile Terahertz Syst. (IWMTS)*, Jul. 2018, pp. 1–6.

[9] F. Sheikh, D. Lessy, M. Alissa, and T. Kaiser, "A comparison study of non-specular diffuse scattering models at terahertz frequencies," in *Proc. 1st Int. Workshop Mobile THz Syst. (IWMTS)*, Duisburg, Germany, 2018, pp. 1–6.

[10] P. Beckmann, "Scattering by non-Gaussian surfaces," *IEEE Trans. Antennas Propag.*, vol. 21, no. 2, pp. 169–175, Mar. 1973.

[11] E. Church and P. Takacs, "Light scattering from non-Gaussian surfaces," *Proc. SPIE*. vol. 2541, pp. 97–107, Sep. 1995, doi: 10.1117/12.218325.

[12] C. Jansen, S. Priebe, C. Moller, M. Jacob, H. Dierke, M. Koch, and T. Kurner, "Diffuse scattering from rough surfaces in THz communication channels," *IEEE Trans. THz Sci. Technol.*, vol. 1, no. 2, pp. 462–472, Nov. 2011.

[13] A. R. Regmi, "Reflection measurement of building materials at microwaves," M.S. thesis, Wireless Commun., Jan. 2016, doi: 10.13140/RG.2.2.21149.51689.

[14] J. Kokkoniemi, J. Lehtomaki, and M. Juntti, "Measurements on rough surface scattering in terahertz band," in *Proc. 10th Eur. Conf. Antennas Propag. (EuCAP)*, Apr. 2016, p. 105.

[15] E. N. Grossman, N. Popovic, R. A. Chamberlin, J. Gordon, and D. Novotny, "Submillimeter wavelength scattering from random rough surfaces," *IEEE Trans. Terahertz Sci. Technol.*, vol. 7, no. 5, pp. 546–562, Sep. 2017.

[16] *Surface texture: Areal—Part 2: Terms, Definitions and Surface Texture*. Accessed: May 21, 2019. [Online]. Available: https://www.iso.org/obp/ui/iso:std:iso:25178:-2:ed-1:v1:en

[17] MountainsMap Software. *3D Surface Texture Analysis and Metrology for Use With Profilometers and Other Surface Measuring Instruments*. Accessed: May 2, 2019. [Online]. Available: https://www.digitalsurf.com

[18] Y. Zhao, G.-C. Wang, and T. M. Lu, *Characterization of Amorphous and Crystalline Rough Surface: Principles and Applications*, vol. 37. Amsterdam, The Netherlands: Elsevier, pp. 241–254, 2001.
[19] J.-J. Wu, "Simulation of rough surfaces with FFT," *Tribol. Int.*, vol. 33, no. 1, pp. 47–58, Jan. 2000. [Online]. Available: http://www.sciencedirect.com/science/article/pii/S0301679X00000165

MAI ALISSA (Student Member, IEEE) received the bachelor's degree in electronics and communications engineering from Damascus University, Syria, in 2011, and the master's degree (Hons.) in advanced optical technologies (Optics in Telecommunication) from Friedrich-Alexander-University Erlangen- Nuremberg, Erlangen, Germany, in 2016. From 2011 to 2013, she worked as a Microwave Planning Engineer with Syriatel, a Mobile Operator. She joined DSV, in January 2017. She worked in different national and European projects, including Wireless 100 Gb/s and beyond, COHERENT- Horizon 2020, and mobile MAteRIal TranscEiver (MARIE). Her current research interests include indoor channel simulation and measurements, and Terahertz in communications.

BENEDIKT FRIEDERICH received the M.S. degree in electrical engineering from the University of Duisburg-Essen, Duisburg, Germany, in 2013, where he is currently pursuing the Ph.D. degree. From 2013 to 2020, he was a Research Assistant with the Chair of Communication Systems, University Duisburg-Essen. His research interests include the digital signal processing for radar applications in terms of synthetic aperture for fire and security applications and especially joint imaging and material characterization techniques. From 2016 to 2020, he is a Fellow of the MARIE project for mobile material characterization and localization by electromagnetic sensing using a mobile THz systems.

FAWAD SHEIKH (Member, IEEE) received the M.Sc. degree in computer science and communication engineering, in 2017, and the Dr.-Ing. degree from the University of Duisburg-Essen, Duisburg, Germany, in 2019. From 2006 to 2011, he worked with Fraunhofer IMS, KlickTel AG, Vodafone D2 GmbH, and Deutsche Telekom AG, respectively, for cellular and IT service management projects. From January 2012 to May 2017, he has been with the Institute of Digital Signal Processing (DSV), University of Duisburg-Essen for the project Wireless 100 Gb/s and beyond. Since June 2017, he has been working on the project mobile MAteRIal TranscEiver (MARIE). He is currently a Postdoctoral Researcher with DSV. His current research interests include systems and components in THz band communication, measurement and modeling of mobile radio channels, massive MIMO systems, and mobile material characterization and localization, within the frequency range of 250 GHz to 4 THz. He is also the Internal Coordinator of the IEEE International Workshop Series on Mobile Terahertz Systems started, in 2018, and the CEO of The Mobile THz Company UG, offering concept designs and performance analyses of Mobile THz Systems.

ANDREAS CZYLWIK received the degree in electrical engineering from the Technical University of Darmstadt, Germany, in 1983, and the Dr.-Ing. and Habilitation degrees in optical communications from the Technical University of Darmstadt, in 1988 and 1994, respectively. From 1994 to 2000, he was with the Research and Development Center (Technologiezentrum) of Deutsche Telekom, Department of Local Area Broadband Radio Systems. He was a Full Professor with the Research Group of Microcellular Radio Systems, Technical University of Braunschweig, in 2000. Since 2002, he has been with the Chair of Communication Systems, University Duisburg-Essen. His research interests include radio communications on link and system level with special focus on adaptive multi-carrier MIMO techniques. Several research activities focus on utilizing high frequency (up to THz) electromagnetic waves with applications in the field of extreme wideband communications and radar systems. He is also interested in the application of radio communications in the field of technical security systems. Since 2014, he has been the Chairman of the European Society for Automatic Alarm Systems (EUSAS).

THOMAS KAISER (Senior Member, IEEE) received the Diploma degree in electrical engineering from Ruhr-University Bochum, Bochum, Germany, in 1991, and the Ph.D. (Hons.) and German Habilitation degrees in electrical engineering from Gerhard Mercator University, Duisburg, Germany, in 1995 and 2000, respectively. From 1995 to 1996, he spent a research leave with the University of Southern California, Los Angeles, CA, USA, which was grantaided by the German Academic Exchange Service. From 2000 to 2001, he was the Head of the Department of Communication Systems, Gerhard Mercator University, Duisburg. From 2001 to 2002, he was the Head of the Department of Wireless Chips and Systems, Fraunhofer Institute of Microelectronic Circuits and Systems, Duisburg. From 2002 to 2006, he was a Co-Leader of the Smart Antenna Research Team, University of Duisburg-Essen, Duisburg. He joined the Smart Antenna Research Group, Stanford University, Stanford, CA, USA, as a Visiting Professor, in 2005. From 2006 to 2011, he was the Head of the Institute of Communication Technology, Leibniz University of Hannover, Hannover, Germany. He joined the Department of Electrical Engineering, Princeton University, Princeton, NJ, USA, as a Visiting Professor, in 2007. He is currently the Head of the Institute of Digital Signal Processing, University of Duisburg-Essen. He is also the Founder and the CEO of ID4us GmbH, Duisburg, an RFID Centric Company. He has authored or coauthored more than 300 articles in international journals and conference proceedings and Ultra Wideband Systems with MIMO (Wiley, 2010) and Digital Signal Processing for RFID (Wiley, 2015). He was the General Chair of the IEEE International Conference on Ultra-Wideband, in 2008, the International Conference on Cognitive Radio Oriented Wireless Networks and Communications, in 2009, the IEEE Workshop on Cellular Cognitive Systems, in 2014, and the IEEE International Workshop on Mobile THz Systems (IWMTS), in 2018 and 2019. He was the Founding Editor-in-Chief of the e-letter of the IEEE Signal Processing Society. He is the Speaker of the Collaborative Research Center Mobile Material Characterization and Localization by Electromagnetic Sensing.